

Neutron and Gamma Ray Multiplicities in Low-Energy Fission of ^{226}Th

A. Kelic,^{1,3} I. M. Itkis,² I. V. Pokrovsky,² E. V. Prokhorova,² B. Benoit,^{1,4} G. Costa,¹
G. G. Chubarian,⁶ L. Donadille,⁵ O. Dorvaux,¹ E. de Goes Brennand,⁴ G. Guillaume,¹
F. Hanappe,⁴ B. Heusch,¹ A. Huck,¹ B.J. Hurst,⁶ M.G. Itkis,² S. Jokic,³ N.A. Kondratiev,²
E.M. Kozulin,² Yu.Ts. Oganessian,² G. Rudolf,¹ A.Ya. Rusanov,² R.P. Schmitt,⁶
L. Stuttge,¹ D. Vorkapic,³ K. Yuasa-Nakagawa¹

*1 IReS, UMR7500, 1N2P3-CNRS/Universite Louis Pasteur, BP28,
F- 67037 Strasbourg Cedex 2, France*

2 Flerov Laboratory of Nuclear Reactions, JINR, Dubna, Moscow region, Russia

3 Vinca Institute of Nuclear Sciences, P.O. Box 522, 11001 Belgrade, Yugoslavia

*4 Universite Libre de Bruxelles, PNTPM, CP229, Avenue F.D. Roosevelt,
BLOSO, Bruxelles, Belgium*

*5 ISN, 1N2P3-CNRS/Universite Joseph Fourier, 53, Avenue des Martyrs,
F- 38026, Grenoble Cedex, France*

6. Texas A&M University, Cyclotron Institute, College Station, TX 77843, USA

Multimodal fission is known for several years in the actinide region. More recently it has also been evidenced for some nuclei in the Th region [1,2]. The mass-energy distributions of fission fragments of the neutron-deficient $^{220,224,226}\text{Th}$ nuclei have been studied in $^{16,18}\text{O} + ^{208}\text{Pb}$ and $^{16}\text{O} + ^{204}\text{Pb}$ reactions at energies below the Coulomb barrier [2]. It was found that the mass distribution is predominantly symmetric but with the decrease of the excitation to about 25 MeV, a shell asymmetric component appears in the form of two shoulders on both sides of the symmetric distribution. The mass distribution is becoming symmetric by moving towards higher neutron deficient.

In this work, we will continue the series of such investigations and reports on the data on pre- and post- fission neutrons and gamma ray multiplicities obtained for the reaction $^{18}\text{O} + ^{208}\text{Pb}$ at $E_{\text{lab}}=78$ MeV as a function of the masses and fragments' energies. This reaction was chosen because its mass yields demonstrate most clearly the competition between the symmetric liquid-drop component, characteristic of heated nuclei created in heavy ion reactions, and the asymmetric shell component predominant in proton and α induced reactions.

Two series of experiments were carried out on VIVITRON accelerator of IReS Strasbourg, France and Tandem INFN Catania, Italy. In both cases we used beam of ^{18}O with a typical intensity of 5 nAp and ^{208}Pb targets of 300 mkg/cm² sandwiched between two 20 mkg/cm²

C layers. Fission fragments were detected with the time-of-flight spectrometers CORSET setup (in Strasbourg, fission fragment and neutron measurements) [3] and DEMAS-3 (in Catania, fission fragment, gamma, and neutron measurements). CORSET spectrometer had two-time-of-flight arms. Each of arms was based on three channel plate position sensitive detectors (one start and two stop detectors) with the typical angular and time resolutions of 0.3 degree and 150 ps respectively. Detectors were installed in a spherical scattering chamber made of 2mm aluminum. DEMAS-3 spectrometer [2] consisted of four large (20x30cm) position sensitive parallel plate avalanche counters where typical angular and time resolutions were 0.5 degree and 250 ps respectively. The γ -ray multiplicities were measured with six 63x63-mm NaI detectors. Detailed description of experimental set-up and procedures are presented in [2,4]. Calibrations and measurements of the energy loss in the target were performed with the help of a ^{252}Cf source.

The neutron detector DEMON [5,6] was used to measure neutrons coinciding with two correlated fission fragments. DEMON consists of 96 NE213 liquid scintillator cells of 20cm length and 16 cm diameter, optically coupled to XP4512B photomultiplier tubes. Neutrons are separated from γ -rays by pulse shape discrimination. Their energy is determined by time of flight measurement over a flight path of typically 180cm. The time resolution was 1.5 ns,

which gives an energy resolution of 4% at 3 MeV. The intrinsic efficiency at this energy is of 50%. Efficiency curves as a function of the energy threshold were obtained by measurements and compared to Monte Carlo simulations [5,6]. The simulation also provides the possibility to estimate the mean interaction depth in the scintillator as a function of the neutron energy, allowing to apply an iterative procedure to obtain a more accurate value of the mean neutron flight path [5]. The detectors in DEMON array were arranged in a cylindrical-like configuration allowing to cover the whole space with a mean distance between two adjacent modules larger than 13 cm, thus with a negligible cross-talk rate. Then the geometrical acceptance amounts to about 5%.

Fig. 1 shows the energy- and angle-integrated mass distribution and the associated pre- and post-fission neutron multiplicities. The asymmetric component appears clearly. The shape of the mass distribution confirms earlier measurements [1,2]. The pre- and post-fission multiplicities and temperatures were extracted by means of a three moving source fit. The whole set of DEMON modules was taken into account for the χ^2 calculation. In a first step, all fission fragments were taken into account regardless of their mass, and six parameters were optimized: ν_{pre} , T_{pre} , ν_{post1} , T_{post1} , and ν_{post2} , T_{post2} . The labels post1 and post2 indicate that in one case the lighter fragment was detected forwards, and the reverse situation in the other case. It was found that neither ν nor T depends on this distinction. Thus, in a second step, T_{post1} and T_{post2} were supposed to be identical, and ν_{post1} and ν_{post2} to be proportional to the mean masses of the respective post fission sources. Therefore a four parameter fit was performed on the three sets of events corresponding respectively to $A=68-98$, $98-128$ and $128-158$. The ν_{pre} and ν_{post} values obtained are presented in Fig.1. Statistical errors on a given parameter have been calculated using the method presented in [7]. Reduced value of χ^2 is 1.07. Systematic errors were not considered since the aim of this measurement was to compare multiplicities in subsets of the data and not to give absolute values. It turns out that pre-fission multiplicity for asymmetric split is about 0.4 units higher

than for the symmetric one. The post fission multiplicities are about 0.5 units larger for the symmetric mass split than for the asymmetric one.

To compare our result with the statistical model predictions, we have performed a Gemini calculation [8] with the standard parameters being used. Delay time of 10^{-18} sec was introduced which is close to the expectations of the statistical model [9] for a system like $^{18}\text{O} + ^{208}\text{Pb}$ at 25 MeV excitation energy. The result of the calculations are presented in Fig. 1 by two lines in case where the level density parameter a is taken equal to 8 or 11. The latter value agrees better with the multiplicity measured for the symmetric component. It is also close to the 10.8 value, which is obtained if one compares the extracted temperature and the excitation energy. On the other hand, the predicted pre-fission multiplicities for the asymmetric component are definitively smaller than the measured ones.

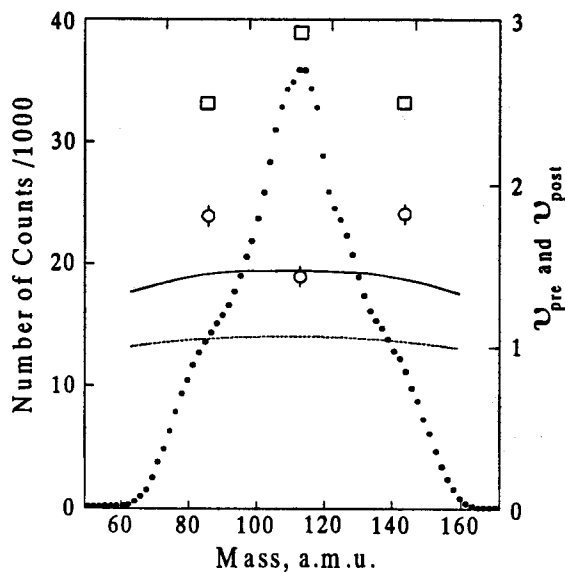


Figure 1. Mass distribution of fission fragments and associated pre- (O) and post- (□) fission neutron multiplicities. The curves indicate the predictions [8] for $a=11$ (full line) and $a=8$ (dashed line).

The observation of an increase of the pre-fission multiplicity with mass asymmetry was unexpected. Clearly, it has to be connected to structure effects, which are seen in the mass distribution and the total kinetic energy of the

fragments [2]. The difference in multiplicity can be interpreted by saying that the time needed to follow the asymmetric valley is longer in case of the symmetric one. It may also mean that the time needed to emit one neutron is shorter. However, it seems unlikely that consideration of the potential energy surface alone will be sufficient to understand the effect. First, this surface is modified by the emission of each pre-fission neutron, so that dynamical calculations are certainly required. Second, structure effects must obviously be taken into account. Because of the particular choice of the compound nucleus and of the very low excitation energy at which it is formed, the present study is the first in which this is demonstrated.

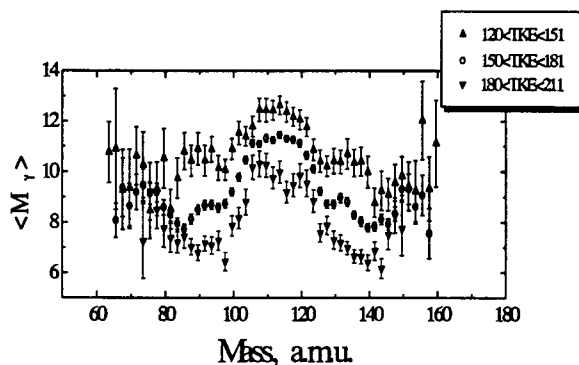


Figure 2. Gamma-ray multiplicities for different TKE cuts.

Observation of higher pre-fission neutron multiplicities and idea of formation of cold fission fragments for asymmetric modes is in a good agreement with conclusions obtained from measurements of γ -ray multiplicities. Figure 2 shows $\langle M_\gamma \rangle$ as a function of the fragment mass for three selected ranges of TKE. For low TKEs, where the input of the asymmetric masses is small, $\langle M_\gamma \rangle$ reaches its highest values, in the mean time the variation of $\langle M_\gamma \rangle$ is the smallest. On the contrary, at the highest TKE where the yield of asymmetric fission fragments is dominating, variation of the $\langle M_\gamma \rangle$ is the largest, but has the lowest absolute value.

Gamma-ray multiplicities as a function of the TKE for different ranges of mass are shown on the fig. 3. For all selected ranges (total, symmetric and asymmetric) $\langle M_\gamma \rangle$ exhibits same

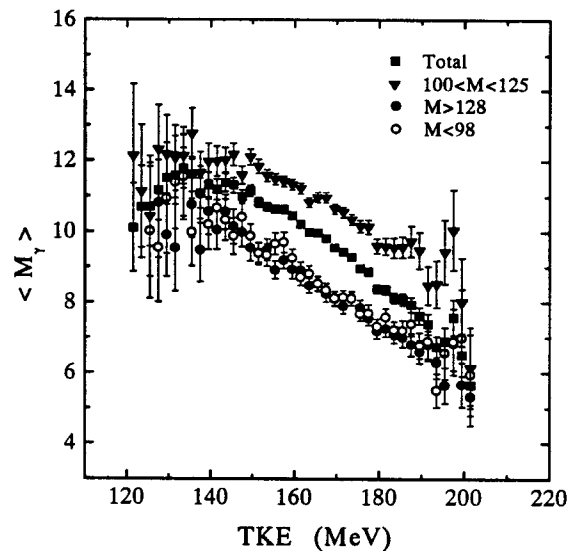


Figure 3. Gamma-ray multiplicities for different mass cuts.

behavior, but absolute values are different. $\langle M_\gamma \rangle$ is approximately 30% higher for symmetric masses than for asymmetric part of the mass distribution, where the influence of shell structure on the fission fragments is the strongest.

Reference:

1. K.H. Schmidt et.al., Phys. Lett. **B325** (1994) 313.
2. M.G. Itkis et.al., Proc of the Tours Symposium on Physics III, Tours, France, 1997, 189 (AIP, Woodbury, New York 1997); Nucl. Phys., in press.
3. E.M. Kozulin et. al., JINR Communication, Dubna **13-95-6**, 1995.
4. G.G. Chubarian et. al., JINR Rapid Communications, **4** (90)-98, 1998, p.21-27.
5. S. Mouatassim et. al., Nucl. Instr. and Meth., **A359** (1995) 330.
6. I. Tilquin et.al., Nucl. Instr. and Meth., **A365** (1995) 446.
7. Ph.R. Bevington, Data Reduction and Error Analysis for the Physical Science. McGraw-Hill Book Company, New York.
8. R.J. Charity et. al., Nucl. Phys., **A483** (1988) 371.
9. D.J. Hind, D. Hilscher and H. Rossner, Nucl. Phys., **A502** (1981) 497c.